




Research Article

The Effect of *G. applanatum* Crude Polysaccharide Extract on Proinflammatory Cytokines and Proapoptotic Caspases in HeLa Cell Line: An *In Vitro* Study

Qurrotu A'yun,¹ Raden Joko Kuncoroningrat Susilo,² Suhailah Hayaza,² Nur'aini Fikriyah,¹ Fina Syifa'una Musthoza,¹ Ufairanisa Islamatasya,¹ Aulia Umi Rohmatika,¹ Dwi Winarni ,³ Sri Puji Astuti Wahyuningsih ,³ Ruey-an Doong,⁴ Deya Karsari,⁵ Aristika Dinar Yanti,⁵ Mochammad Zakki Fahmi,⁶ and Win Darmanto ^{3,7}

¹Magister Program in Biology, Faculty of Science and Technology, Universitas Airlangga, Surabaya 60115, Indonesia

²Department of Nanotechnology Engineering, Faculty of Advance Technology and Multidiscipline, Universitas Airlangga, Surabaya 60115, Indonesia

³Department of Biology, Faculty of Science and Technology, Universitas Airlangga, Surabaya 60115, Indonesia

⁴Institute of Analytical and Environmental Sciences, National Tsing Hua University, Sec. 2 Kuang Fu Road, Hsinchu 30013, Taiwan

⁵Stem Cell Research and Development Center, Universitas Airlangga, Surabaya 60115, Indonesia

⁶Department of Chemistry, Faculty of Science and Technology, Universitas Airlangga, Surabaya 60115, Indonesia

⁷Institute of Science Technology and Health, Jombang 61419, Indonesia

Correspondence should be addressed to Win Darmanto; windarmanto@fst.unair.ac.id

Received 13 January 2023; Revised 20 August 2023; Accepted 26 August 2023; Published 19 September 2023

Academic Editor: Der Jiun Ooi

Copyright © 2023 Qurrotu A'yun et al. This is an open access article distributed under the Creative Commons Attribution License, which permits unrestricted use, distribution, and reproduction in any medium, provided the original work is properly cited.

Polysaccharide extracts exhibit promise as potential anticancer agents. Among the fungi rich in polysaccharide content, *G. applanatum* stands out; however, its anticancer activity necessitates further investigation. This study aims to explore the impact of *G. applanatum* crude polysaccharide (GACP) extract by assessing its effects on cell viability, levels of proinflammatory cytokines such as TNF- α , IFN- γ , IL-2, and IL-12, and levels of proapoptotic markers including caspase-3 and caspase-9, as well as the percentages of necrosis and apoptosis in the HeLa cell line. Employing the HeLa cell line as a research model, four groups were studied: KN (media and DMSO), K+ (doxorubicin 10 $\mu\text{g}/\text{mL}$), P1 (*G. applanatum* extract 200 $\mu\text{g}/\text{mL}$), and P2 (*G. applanatum* extract 400 $\mu\text{g}/\text{mL}$). The *G. applanatum* extract was obtained via boiling distilled water. Anticancer activity was evaluated through the MTT test (3-(4,5-dimethylthiazole-2-yl)-2,5-diphenyltetrazolium bromide) conducted over three treatment durations (24, 48, and 72 hours). Cytokine levels and caspase-3 and caspase-9 levels were assessed using the ELISA test. Cell apoptosis was determined using the Annexin V-PI biomarker and analyzed through flow cytometry. The MTT test exhibited optimal results at the 48-hour treatment mark. Cytokine level analysis revealed significant reductions in TNF- α , IFN- γ , IL-2, and IL-12 levels ($p < 0.005$). Concurrently, caspase-3 and caspase-9 levels exhibited substantial increases ($p < 0.005$). Flow cytometry highlighted the highest percentage of apoptosis in HeLa cells. In conclusion, *G. applanatum*'s polysaccharide extract demonstrates potential as an anticancer and therapeutic agent for cancer treatment.

1. Introduction

Cancer is the second leading cause of death worldwide [1], with cervical cancer displaying an escalating incidence, particularly prominent in Indonesia. Cervical cancer, primarily induced by human papillomavirus (HPV) infection, notably HPV16 and HPV18 [2–4], is influenced by diverse factors encompassing genetics, dietary habits, oxidative stress, environmental toxins, and psychological stress [5–7]. While early-stage cervical cancer may remain asymptomatic, advanced stages manifest symptoms such as vaginal bleeding, ureteral obstruction, hydronephrosis, uremia, and pericarditis [8–11]. The significance of proinflammatory cytokines lies in their role as stimulators in phosphorylating the inhibitor of κ B (IKK) complex, a pivotal step in translocating NF- κ B to the nucleus [12–16]. Subsequently, NF- κ B engages in transcription, yielding proinflammatory cytokines that foster cancer cell survival. Current treatment modalities for cervical cancer span surgery, chemotherapy, and radiotherapy [17, 18], yet their efficacy is hampered by considerable side effects and susceptibility to relapse [12].

Consequently, the quest for efficacious, affordable, and nontoxic cancer treatments intensifies, fostering interest in exploring natural sources such as *G. applanatum*. This particular fungus features in pharmacological studies, gaining prominence within traditional Chinese medicine due to its attributed medicinal properties spanning anticancer, antidiabetic, antifibrotic, and anti-inflammatory effects [13–16]. *G. applanatum* comprises diverse bioactive constituents, notably polysaccharides and triterpenoids [19–24]. Polysaccharides' biological activity correlates closely with factors such as sulfate content, molecular weight, and glycosidic bond type [25, 26]. Low molecular weight polysaccharides exhibit anticancer potential against various tumor types. Notably, *G. applanatum*'s polysaccharide content demonstrates antimicrobial, antioxidant, anti-inflammatory, and antitumor properties [27–30]. Existing research underscores polysaccharides' role in regulating cell cycle, apoptosis, and autophagy in cancer [31–33]. However, the specific impact of *G. applanatum* polysaccharides on cancer cells through the apoptosis pathway remains an area warranting exploration. This study delves into the influence of *G. applanatum* crude polysaccharide (GACP) extract on proinflammatory cytokines and its induction of apoptosis in HeLa cells.

2. Materials and Methods

2.1. *G. applanatum* Crude Polysaccharide Extract Preparation. *G. applanatum* specimens were sourced from Tulungagung, East Java, Indonesia. The extraction procedure, as detailed by Susilo et al. [14], was pursued. Dr. Ni'matuzzahroh conducted the identification based on a designated key book [19]. In essence, the basidiocarp of *G. applanatum* was sectioned and air-dried, after which the dried segments were milled into a fine powder. The powdered material was weighed and subjected to boiling at temperatures between 90 and 100°C for a duration of 6 hours. Following the boiling phase, the filtrate extracted from *G. applanatum* underwent

centrifugation at 4300 rpm for 5 minutes. The resulting supernatant was precipitated using absolute ethanol in a 1 : 3 ratio. This precipitation process was reiterated three times, and the ensuing pellets were isolated. The pellets were subsequently dissolved in distilled water and again subjected to centrifugation, following the same approach. The resultant pellets were freeze-dried to yield the GACP extract.

2.2. FTIR Analysis. For FTIR analysis, the GACP extract was incorporated into potassium bromide (KBr) pellets and assessed using the Nicolet™ iS20 FTIR Spectrometer.

2.3. HeLa Cell Culture. HeLa cells were procured from Stem Cell Research and Development at Universitas Airlangga. The cells were cultivated in DMEM and incubated at a temperature of 37°C in an atmosphere containing 5% CO₂. The administration of GACP extract was undertaken based on specific concentrations allocated to each group, facilitated by a DMSO solvent at levels below 1%. The treatment doses applied in this investigation encompassed the K⁻ group (negative control: media + HeLa cell line), K⁺ group (positive control: HeLa cell line + 10 µg/mL doxorubicin), P1 group (HeLa cell line + GACP 200 µg/mL), and P2 group (HeLa cell line + GACP 400 µg/mL). Cells were subsequently cultured for durations of 24, 48, and 72 hours before being harvested to facilitate further assessments.

2.4. Cell Viability. The evaluation of HeLa cell viability entailed the utilization of the MTT technique (3-(4,5-dimethylthiazole-2-yl)-2,5-diphenyltetrazolium bromide) [34]. Cells procured from the CO₂ incubator underwent meticulous examination to confirm their uncontaminated status. For cell harvest, cultures achieving an 80% confluence were selected. Postharvest, cell enumeration, and subsequent dilution with complete culture medium occurred. The cells were then dispensed into a 96-well plate, allotting 5 × 10³ cells to each well, followed by overnight incubation. Varied concentrations of GACP extract (200 µg/mL and 400 µg/mL) were introduced, employing DMSO as a cosolvent. This assembly was then incubated in a 37°C, 5% CO₂ incubator for a duration of 24 hours. At the conclusion of incubation, 100 µL of MTT reagent (0.5 mg/mL) dissolved in DMEM was appended to each well. A subsequent 3-hour incubation at 37°C ensued, resulting in the formation of formazan. The cellular examination was conducted employing an inverted microscope. Subsequent to the distinct appearance of formazan, the introduction of a 10% SDS halt solution in 0.1 N HCl took place. The plate, enveloped in aluminum foil, was relegated to an obscure setting overnight. The optical density (OD) values were gauged via a microplate reader at a wavelength of 595 nm.

2.5. Cytokine Levels Analysis. ELISA kits (Bioassay Technology, Shanghai, China) facilitated the quantification of cytokine levels in accordance with the manufacturer's stipulations. Each well of a well plate received a total of 40 L of HeLa cell supernatant. Sequentially, 10 µL and 50 µL of

streptavidin-HRP antibodies were incorporated. A 60-minute incubation at 37°C followed, succeeded by five washes with washing buffer. Subsequently, 50 μ L of substrate solutions A and B were individually introduced to each well. An additional 10-minute incubation at 37°C under dark conditions ensued. Termination involved the addition of 50 μ L of stop solution to each well. This treatment was executed across six replications. Within a span of less than 10 minutes, the optical density (OD) values were recorded through an ELISA reader (Thermo Scientific™ Multiskan™ GO Microplate Spectrophotometer) at a wavelength of 450 nm.

2.6. Caspase Levels Analysis. Caspase-3 and caspase-9 levels were assessed through the utilization of an ELISA kit (Bioassay Technology, Shanghai, China), adhering to the provided manufacturing protocol. Each well plate was allocated a total of 40 L of supernatant originating from HeLa cell cultures. Subsequent to this, mouse antibody caspase-3 was introduced for the quantification of caspase-3 levels, while mouse antibody caspase-9 was employed for the evaluation of caspase-9 levels. A sequential addition of 50 L of streptavidin-HRP followed, culminating in an 1-hour incubation at room temperature. Following this, a thrice-repeated washing step was undertaken using a washing buffer. Successively, 50 L of substrate A solution was dispensed into each well plate. Subsequently, substrate B was introduced and incubated in the dark at 37°C for a duration of 10 minutes. The conclusion of this process involved the addition of 50 L of stop solution. This treatment was executed across six replications. Measurement occurred via an ELISA reader (Thermo Scientific™ Multiskan™ GO Microplate Spectrophotometer) at a wavelength of 450 nm.

2.7. Apoptosis Index. The detection of apoptosis was executed through flow cytometry [35]. In 6-well plates, a total of 1×10^5 HeLa cells were subjected to incubation with *G. applanatum* extract and medium under 5% CO₂ at 37°C overnight. Subsequent to this incubation, the mixture of *G. applanatum* extract and medium was withdrawn. The addition of a solution composed of PBS, EDTA, and trypsin transpired in each well, followed by a 2-minute incubation within the CO₂ incubator. The aspirates from each well were then combined in Eppendorf tubes and centrifuged at 2500 rpm for 5 minutes. Postcentrifugation, cells within each Eppendorf were subjected to a cold PBS wash, followed by centrifugation at 1500 rpm at 4°C. A suspension of 400 L binding buffer incorporating 5 L annexin V-FITC and 10 L PI was prepared, and a 10-minute incubation at 4°C in darkness ensued. This treatment was executed across six replications. This protocol was replicated six times. Flow cytometry analysis was undertaken using guava® Flow Cytometry easyCyte™ Systems.

2.8. Statistical Analysis. All data were presented as mean \pm SD and subsequently subjected to analysis using GraphPad Prism software version 8 (San Diego, CA, USA).

The one-way ANOVA test was employed to ascertain the significance of GACP extract impact. Following this, the Tukey test was administered to highlight significant disparities between groups. A statistical significance threshold was established at $p < 0.05$.

3. Results

3.1. FTIR Analysis. The FTIR analysis results are depicted in Figure 1. The analysis unveiled the existence of multiple functional groups through the observation of a total of 41 peaks. Notably, a robust peak at 1631.14 cm^{-1} , indicative of C=C stretching, signifies the presence of alkenes within the GACP extracts. In addition, a peak at 1399.73 cm^{-1} , corresponding to C-H stretching, suggested the existence of alkanes within the GACP extracts. Moreover, a pronounced peak at 1004.48 cm^{-1} , denoting the C-O bending mode, highlighted the presence of compounds such as alcohols, carboxylic acids, esters, and ethers. Furthermore, a range of peaks spanning from 3970.97 cm^{-1} to 1884.09 cm^{-1} showcased various functional groups, including alcohol (O-H stretching), amine (N-H stretching), carboxylic acid (O-H stretching), alkane (C-H stretching), alkyne (C=C stretching), and allene (C=C=C stretching).

3.2. Cell Viability. The percentage of cell viability is illustrated in Figure 2. The outcomes exhibited a reduction in cell viability with increasing doses of GACP extracts. Notably, the administration of GACP extracts for 24 hours resulted in viabilities of 62.46% at 50 $\mu\text{g/mL}$, 56.60% at 100 $\mu\text{g/mL}$, 51.90% at 200 $\mu\text{g/mL}$, 45.51% at 400 $\mu\text{g/mL}$, and 39.80% at 800 $\mu\text{g/mL}$. In addition, at 48 hours, cell viability percentages were recorded as 126.99% at 50 $\mu\text{g/mL}$, 53.15% at 100 $\mu\text{g/mL}$, 46.07% at 200 $\mu\text{g/mL}$, 43.57% at 400 $\mu\text{g/mL}$, and 40.09% at 800 $\mu\text{g/mL}$. Furthermore, the cell viability percentages at 72 hours demonstrated values of 102.52% at 50 $\mu\text{g/mL}$, 76.52% at 100 $\mu\text{g/mL}$, 66.20% at 200 $\mu\text{g/mL}$, 54.86% at 400 $\mu\text{g/mL}$, and 39.02% at 800 $\mu\text{g/mL}$.

3.3. Apoptotic Index. The apoptotic index is illustrated in Figure 3. In the normal control group (A), live cells constituted 56.6%, early apoptosis was 3.3%, final apoptosis reached 25.1%, and necrosis accounted for 14.9%. In the positive control group (B), live cells were at 27.8%, early apoptosis was 12.2%, final apoptosis was 58.9%, and necrosis was minimal at 1.1%. For the treatment group with GACP extract 200 $\mu\text{g/mL}$ (C), live cells were 39.2%, early apoptosis accounted for 3.4%, final apoptosis was 45.6%, and necrosis was 11.9%. Similarly, in the treatment group with GACP extract 400 $\mu\text{g/mL}$ (D), live cells constituted 28.4%, early apoptosis was 4.3%, final apoptosis reached 56.1%, and necrosis was 11.2%.

3.4. Effect of *G. applanatum* Extract on Proinflammatory Cytokine. Figure 4 presents the effect of *G. applanatum* extract on proinflammatory cytokine levels. Specifically, TNF- α levels were measured at $65.80 \pm 8.25 \mu\text{g/mL}$ for K-

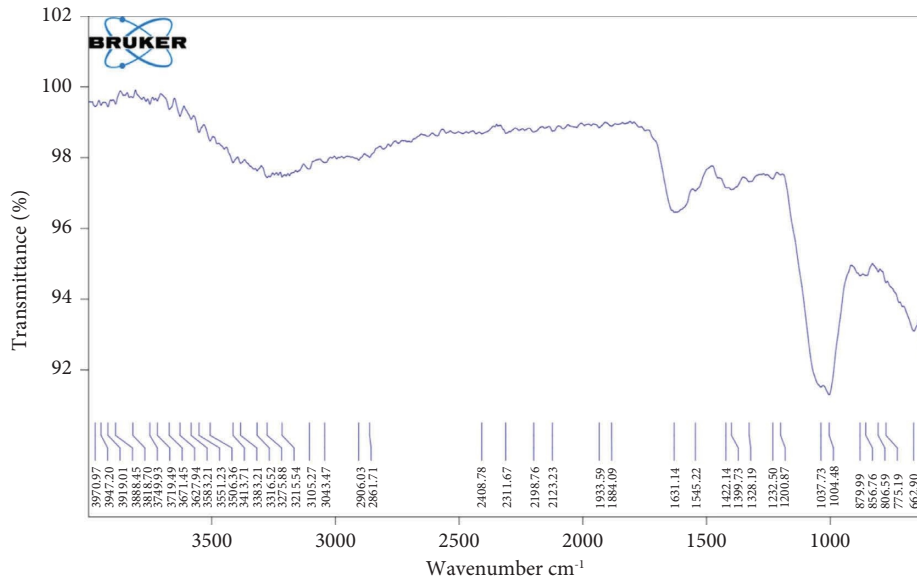


FIGURE 1: FTIR analysis of *G. applanatum* crude polysaccharide extracts.

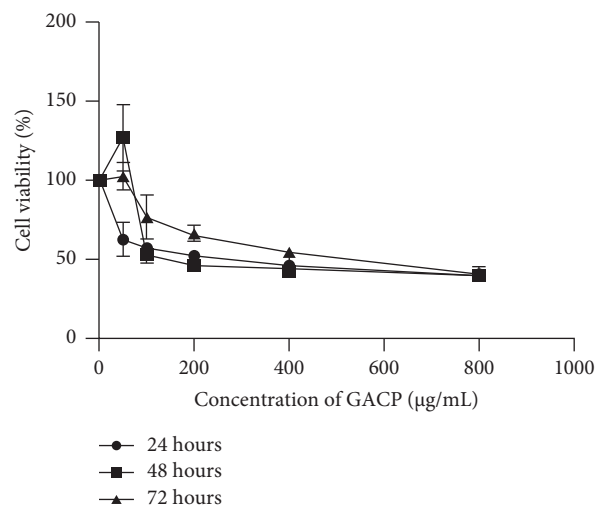


FIGURE 2: Effect of *G. applanatum* crude polysaccharide extracts on cell viability of HeLa cells. *G. applanatum* crude polysaccharide extracts with various concentrations were treated at three incubation times (24, 48, and 72 hours).

$11.86 \pm 7.18 \mu\text{g/mL}$ for K^+ , $19.41 \pm 1.42 \mu\text{g/mL}$ for P1, and $15.58 \pm 5.32 \mu\text{g/mL}$ for P2. For $\text{IFN-}\gamma$, levels were $5.09 \pm 0.27 \mu\text{g/mL}$ for K^- , $3.05 \pm 0.60 \mu\text{g/mL}$ for K^+ , $3.08 \pm 0.46 \mu\text{g/mL}$ for P1, and $3.16 \pm 0.38 \mu\text{g/mL}$ for P2. Correspondingly, IL-2 levels were found to be $3.88 \pm 0.66 \mu\text{g/mL}$ for K^- , $2.54 \pm 0.13 \mu\text{g/mL}$ for K^+ , $2.60 \pm 0.20 \mu\text{g/mL}$ for P1, and $2.57 \pm 0.38 \mu\text{g/mL}$ for P2. In addition, IL-12 levels were $3.46 \pm 0.04 \mu\text{g/mL}$ for K^- , $2.38 \pm 0.63 \mu\text{g/mL}$ for K^+ , $2.62 \pm 0.55 \mu\text{g/mL}$ for P1, and $3.21 \pm 0.06 \mu\text{g/mL}$ for P2. Importantly, in the positive group and GACP-treated groups, parameters such as $\text{TNF-}\alpha$ levels, $\text{IFN-}\gamma$ levels, IL-2 levels, and IL-12 levels were significantly ($p < 0.05$) lower than those in the negative control group. The administration of GACP extract effectively mitigated the increase in $\text{TNF-}\alpha$ levels, $\text{IFN-}\gamma$ levels, IL-2 levels, and IL-12 levels when compared to the negative control group. These

results indicated that the GACP extract effectively played a protective role against cancer. Comparative analysis between the effects of doxorubicin and GACP extract on proinflammatory cytokine parameters demonstrated that doxorubicin had a lower impact than GACP extract on HeLa cells. Nevertheless, GACP extract exhibited significant effects compared to the negative control group, affirming its potential as an anticancer agent.

3.5. Effect of *G. applanatum* Extract on Caspase-9 and Caspase-3. Figure 5 illustrates the impact of *G. applanatum* extract on caspase-9 and caspase-3 levels. Regarding caspase-3 levels, values were found to be $3.60 \pm 0.42 \mu\text{g/mL}$ for K^- , $7.61 \pm 1.87 \mu\text{g/mL}$ for K^+ , $6.012 \pm 1.173 \mu\text{g/mL}$ for P1, and $6.88 \pm 0.96 \mu\text{g/mL}$ for P2. On the other hand, for

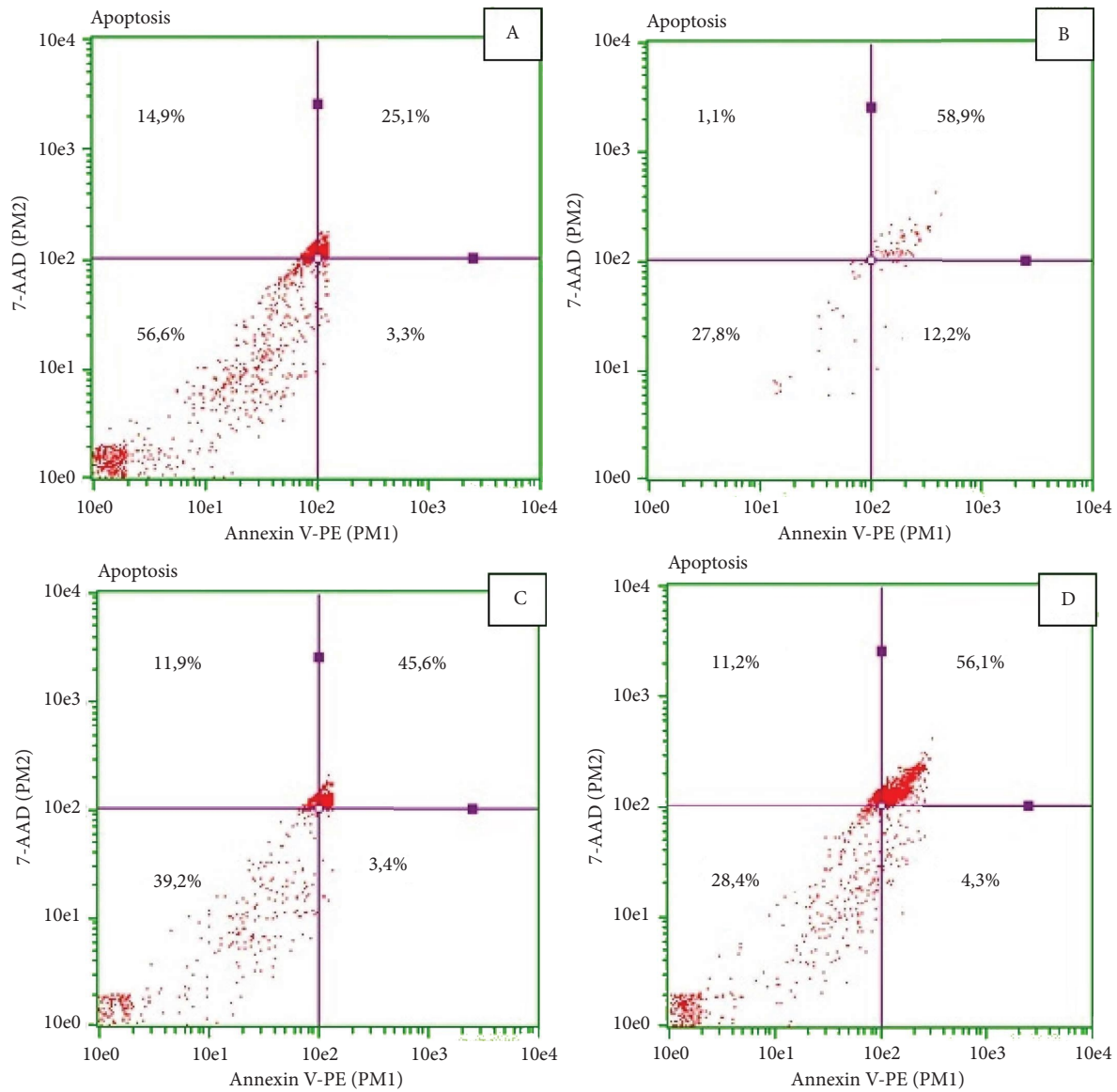


FIGURE 3: Effect of *G. applanatum* crude polysaccharide extracts on apoptotic index by flow cytometry test. (a) K- group; (b) K+ group; (c) P1 group; (d) P2 group. Bottom left: live cells; bottom right: early apoptosis; top right: late apoptosis; top left: necrosis.

caspase-9, the levels were $1.73 \pm 0.22 \mu\text{g/mL}$ for K-, $5.67 \pm 1.62 \mu\text{g/mL}$ for K+, $4.05 \pm 0.34 \mu\text{g/mL}$ for P1, and $4.105 \pm 0.37 \mu\text{g/mL}$ for P2. These ELISA assay results strongly indicate that GACP significantly increased caspase-9 and caspase-3 levels, implying that GACP potentially induced apoptosis through the classical nuclear DNA damage pathways. Notably, the expression of caspase-9 and caspase-3 in the GACP-treated groups and the positive control group was significantly ($p < 0.05$) higher than that in the negative control group. When comparing the effects of doxorubicin and GACP extract on caspase levels, substantial differences were observed. Doxorubicin led to higher increases in caspase-9 and caspase-3 levels than those in the GACP-treated groups. Nevertheless, the administration of GACP extract significantly increased caspase-9 and caspase-3 levels, underscoring its role in apoptosis induction and affirming its potential as an anticancer agent.

4. Discussion

The utilization of natural sources as a safe approach for drug development, especially in cancer treatment, has gained prominence. In this study, GACP was administered to HeLa cells to assess cell viability. The results of GACP exposure over 24, 48, and 72 hours exhibited varying percentages of cell viability. Notably, the 72-hour exposure yielded higher cell viability percentages compared to 24 and 48 hours at higher doses. This condition could be attributed to cell adaptation in HeLa cells. Extended exposure to GACP, such as at 72 hours, may have facilitated cell survival and replication. The findings suggest that GACP does not exert toxic effects on HeLa cells. Chronic conditions often lead to increased levels of proinflammatory cytokines. In the case of HeLa cells, they produce proinflammatory cytokines such as TNF- α , IL-6, IL-2, IL-12, and IFN- γ to sustain tumor

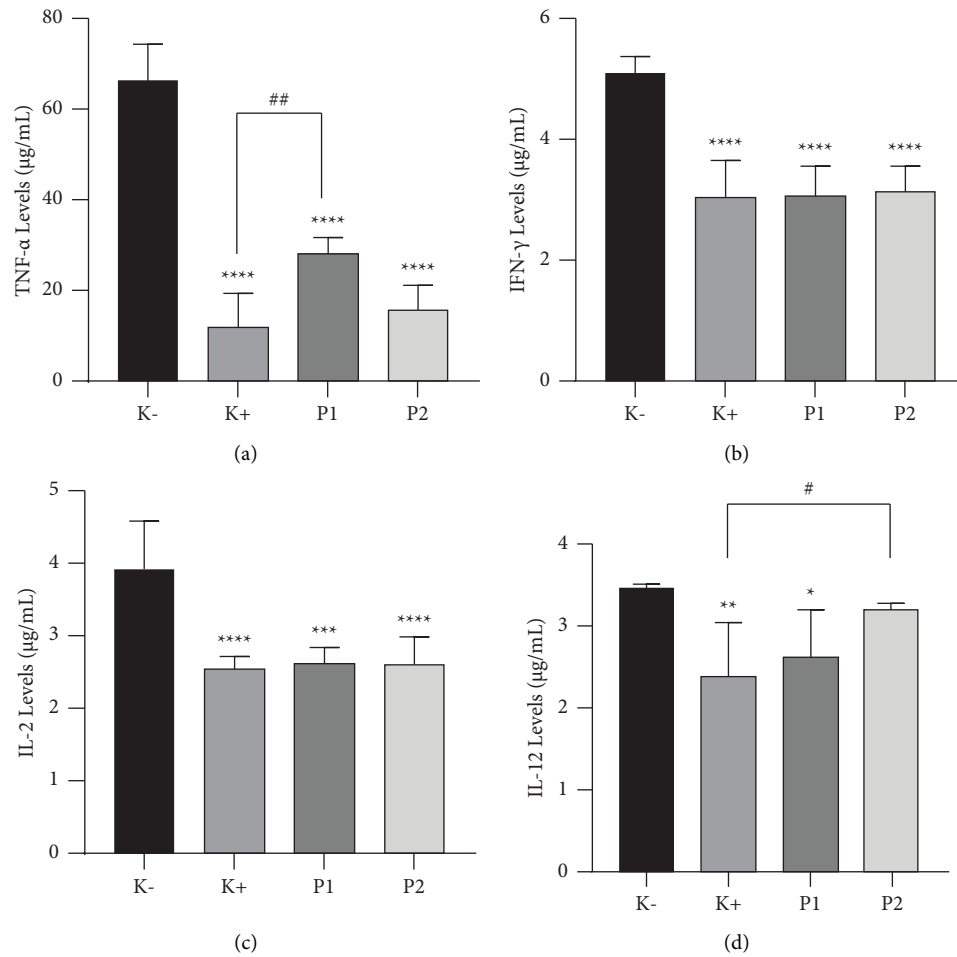


FIGURE 4: Effect of *G. applanatum* crude polysaccharide extracts on proinflammatory cytokine parameters. (a) TNF- α levels, (b) IFN- γ levels, (c) IL-2 levels, and (d) IL-12 levels. Data are presented as mean \pm SD ($n=6$). **** $p < 0.0001$ compared to the negative group (K-). *** $p < 0.001$ compared to the negative group (K-). ** $p < 0.01$ compared to the negative group (K-). * $p < 0.05$ compared to the negative group (K-). ## $p < 0.01$ compared to the positive group (K+). # $p < 0.05$ compared to the positive group (K+). K-: negative control; K+: positive control; P1: *G. applanatum* crude polysaccharide extract 100 $\mu\text{g}/\text{mL}$; P2: *G. applanatum* crude polysaccharide extract 200 $\mu\text{g}/\text{mL}$. TNF- α : tumor necrosis factor- α , IFN- γ : interferon- γ , IL-2: interleukin-2, and IL-12: interleukin-12.

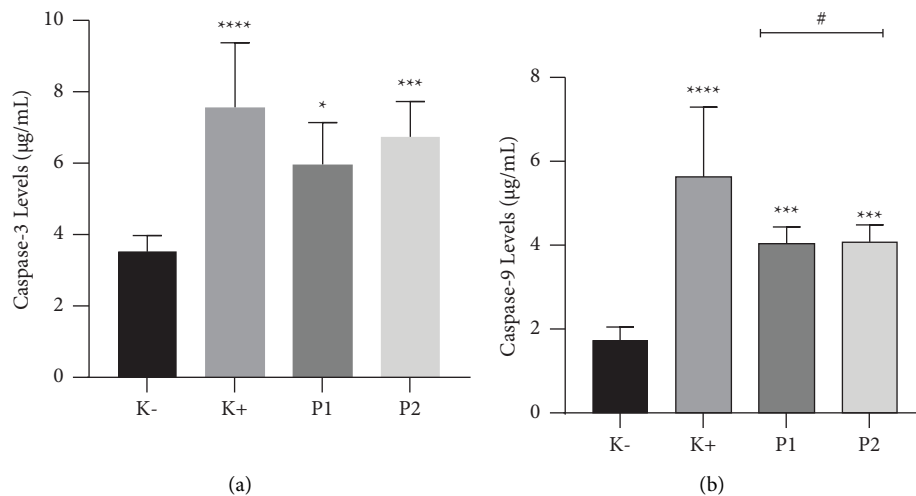


FIGURE 5: Effect of *G. applanatum* crude polysaccharide extracts on caspase-9 and caspase-3 levels. (a) Caspase-3 levels, (b) caspase-9 levels. Data are presented as mean \pm SD ($n=6$). **** $p < 0.0001$ compared to the negative group (K-). *** $p < 0.001$ compared to the negative group (K-). * $p < 0.05$ compared to the negative group (K-). # $p < 0.05$ compared to the positive group (K+). K-: negative control; K+: positive control; P1: *G. applanatum* crude polysaccharide extract 100 $\mu\text{g}/\text{mL}$; P2: *G. applanatum* crude polysaccharide extract 200 $\mu\text{g}/\text{mL}$.

development and proliferation over the long term [36, 37]. Moreover, proinflammatory cytokines can drive angiogenesis and metastasis within the tumor microenvironment [21, 38]. The activation of NF- κ B is a critical factor in promoting proinflammatory cytokine abundance. The prevention of NF- κ B activation has become a significant focus in the field of cancer treatment. In this study, GACP demonstrated the ability to decrease levels of TNF- α , IL-6, IL-2, IL-12, and IFN- γ . The polysaccharides present in GACP are thought to inhibit IK β phosphorylation, thereby hindering the translocation of NF- κ B. This mechanism ultimately results in lower proinflammatory cytokine production by HeLa cells [22, 39].

The study also explored the impact of GACP on the apoptosis pathway in HeLa cells. The decrease in proinflammatory cytokine levels contributed to a reduced survival rate of HeLa cells, thereby initiating the apoptosis process [40–42]. This study aims to examine GACP effects in apoptosis, measured by flow cytometry. The use of Annexin V-FITC allowed for the detection of early apoptosis, as it can identify phospholipid phosphatidylserine (PS) exposed on the outer plasma membrane. In addition, propidium iodide (PI) was employed to stain nuclear DNA, enabling the identification of late apoptosis and necrosis following the loss of cell membrane integrity. The dose of 400 μ g/mL of GACP exhibited the highest percentage of late apoptosis at 48 hours. However, the optimal dose was found to be 200 μ g/mL at 24 hours, as it led to 39.2% viable cells without inducing cell toxicity while still inducing apoptosis in 45.6% of HeLa cells. Notably, the percentage of early apoptosis induced by doxorubicin was higher than that induced by GACP treatment or the control group. This suggests that GACP holds potential as an anticancer agent, particularly in triggering late apoptosis. Furthermore, the study elucidated the underlying mechanism of GACP-induced apoptosis, particularly through the intrinsic pathway. The treatment with GACP led to elevated levels of caspase-9 and caspase-3 compared to the control group. Caspase-9, known as an initiator caspase, plays a pivotal role in activating executor caspases, such as caspase-3 [43–45]. Apoptosis is initiated by an increase in proapoptotic proteins like BAX, BAK1, BIM, BID, and BBC3, which stimulate mitochondria to release cytochrome c into the cytoplasm. This triggers the formation of the apoptosome and activation of caspase-3 [25]. The apoptosome forms when cytochrome c binds to Apaf-1, followed by the subsequent joining of procaspase-9 to the apoptosome, leading to its cleavage and activation. The activation of caspase-9 further stimulates the activation of caspase-3 [26], which orchestrates apoptosis by cleaving and activating proteins crucial for the proteolytic degradation of cancer cells. Ultimately, this process leads to the elimination of cancer cells and the suppression of tumor growth. The enhancement of caspase-9 and caspase-3 production suggests that GACP holds potential as an anticancer agent, particularly for the treatment of cervical cancer.

Previous studies have underscored the potential therapeutic effects of *G. applanatum* crude extract in cervical

cancer treatment. These effects include inducing apoptosis via the intrinsic pathway, inhibiting DNA survival and transcription factor proliferation, causing DNA fragmentation, and curbing the growth and metastatic potential of cervical cancer cells [46]. The existing literature on *G. applanatum*'s anticancer properties further solidifies its potential in cancer therapy, including its toxicity against tumor cells compared to normal cells [47].

5. Conclusion

In conclusion, the polysaccharide compounds obtained from *G. applanatum* have the capability to induce apoptosis in HeLa cells by upregulating the levels of caspase-3 and caspase-9. However, to gain a deeper understanding of the underlying molecular mechanisms driven by *G. applanatum* extract, further investigations are warranted. Further research should prioritize the analysis of protein interactions, protein signaling, and regulatory factors implicated in apoptotic responses, particularly through animal studies (*in vivo*).

Abbreviations

| | |
|-----------------|--|
| PBS: | Phosphate-buffered saline |
| EDTA: | Ethylenediaminetetraacetic acid |
| BAX: | Bcl-2-associated X protein |
| BCL-2: | B-cell lymphoma 2 |
| BAK 1: | Bcl-2 homologous antagonist killer |
| BIM: | Bcl-2-interacting mediator of cell death |
| BID: | BH3-interacting domain death agonist |
| BBC3: | Bcl-2 binding component 3 |
| ELISA: | Enzyme-linked immunosorbent assay |
| DMEM: | Dulbecco's modified Eagle medium |
| TNF- α : | Tumor necrosis factor-alpha |
| IFN- γ : | Interferon-gamma |
| IL-2: | Interleukin-2 |
| IL-6: | Interleukin-6 |
| IL-12: | Interleukin-12 |
| FTIR: | Fourier transform infrared |
| NF- κ B: | Nuclear factor kappa B |
| Apaf-1: | Apoptotic protease activating factor-1. |

Data Availability

The data used to support the study are included within the article.

Conflicts of Interest

The authors declare that there are no conflicts of interest related to the publication of this paper.

Authors' Contributions

WD, RJKS, and SH designed the study; WD, DW, and SPAW wrote ethical and experiment protocol; QA, NF, FSM, DK, ADY, and MZF carried out laboratory examination; QA, RJKS, and SH performed statistical analysis; QA, RJKS, SH, UI, and AUR drafted the manuscript; and WD

and RD supervised the project. All authors contribute to the manuscript and approved the final version of the manuscript.

Acknowledgments

The authors would like to extend their gratitude to Dr. Nimatuzahroh from the Department of Biology for her contribution to providing taxonomic identification of *G. applanatum*. This work was supported by Mandat Research Grant 2021 from Universitas Airlangga.

References

- [1] H. Nagai and Y. H. Kim, "Cancer prevention from the perspective of global cancer burden patterns," *Journal of Thoracic Disease*, vol. 9, no. 3, pp. 448–451, 2017.
- [2] S. Zhang, H. Xu, L. Zhang, and Y. Qiao, "Cervical cancer: epidemiology, risk factors and screening," *Chinese Journal of Cancer Research*, vol. 32, no. 6, pp. 720–728, 2020.
- [3] X. Wang, X. Huang, and Y. Zhang, "Involvement of human papillomaviruses in cervical cancer," *Frontiers in Microbiology*, vol. 9, no. 11, pp. 2896–2914, 2018.
- [4] C. K. Chan, G. Aimagambetova, T. Ukybassova, K. Kongrtay, and A. Azizan, "Human papillomavirus infection and cervical cancer: epidemiology, screening, and vaccination- review of current perspectives," *Journal of Oncology*, vol. 2019, Article ID 3257939, 11 pages, 2019.
- [5] A. Singh, R. Kukreti, L. Saso, and S. Kukreti, "Oxidative stress: a key modulator in neurodegenerative diseases," *Molecules*, vol. 24, no. 8, pp. 1583–1620, 2019.
- [6] E. B. Kurutas, "The importance of antioxidants which play the role in cellular response against oxidative/nitrosative stress: current state," *Nutrition Journal*, vol. 15, no. 1, pp. 71–22, 2016.
- [7] H. Jin, C. Song, Z. Zhao, and G. Zhou, "Ganoderma lucidum polysaccharide, an extract from ganoderma lucidum, exerts suppressive effect on cervical cancer cell malignancy through mitigating epithelial-mesenchymal and JAK/STAT5 signaling pathway," *Pharmacology*, vol. 105, no. 7–8, pp. 461–470, 2020.
- [8] U. Asmat, K. Abad, and K. Ismail, "Diabetes mellitus and oxidative stress—a concise review," *Saudi Pharmaceutical Journal*, vol. 24, no. 5, pp. 547–553, 2016.
- [9] M. Sharifi-Rad, N. V. Anil Kumar, P. Zucca et al., "Lifestyle, oxidative stress, and antioxidants: back and forth in the pathophysiology of chronic diseases," *Frontiers in Physiology*, vol. 11, no. 7, pp. 694–721, 2020.
- [10] G. U. Eleje, A. C. Eke, G. O. Igberase, A. O. Igwegbe, and L. I. Eleje, "Palliative interventions for controlling vaginal bleeding in advanced cervical cancer," *Cochrane Database of Systematic Reviews*, vol. 3, no. 3, Article ID 11000, 2019.
- [11] T. Zhang, C. Ma, Z. Zhang, H. Zhang, and H. Hu, "NF- κ B signaling in inflammation and cancer," *MedComm*, vol. 2, no. 4, pp. 618–653, 2021.
- [12] R. Chhabra, "Cervical cancer stem cells: opportunities and challenges," *Journal of Cancer Research and Clinical Oncology*, vol. 141, no. 11, pp. 1889–1897, 2015.
- [13] S. Zhou, S. Guan, Z. Duan et al., "Molecular cloning, codon-optimized gene expression, and bioactivity assessment of two novel fungal immunomodulatory proteins from *Ganoderma applanatum* in *Pichia*," *Applied Microbiology and Biotechnology*, vol. 102, no. 13, pp. 5483–5494, 2018.
- [14] R. J. K. Susilo, D. Winarni, S. Hayaza, R. A. Doong, S. P. A. Wahyuningsih, and W. Darmanto, "Effect of crude *Ganoderma applanatum* polysaccharides as a renoprotective agent against carbon tetrachloride-induced early kidney fibrosis in mice," *Veterinary World*, vol. 15, no. 4, pp. 1022–1030, 2022.
- [15] M. F. Ahmad, "Ganoderma lucidum: persuasive biologically active constituents and their health endorsement," *Biomedicine & Pharmacotherapy*, vol. 107, no. 4, pp. 507–519, 2018.
- [16] M. S. Hossain, A. Barua, M. A. H. Tanim et al., "Ganoderma applanatum mushroom provides new insights into the management of diabetes mellitus, hyperlipidemia, and hepatic degeneration: a comprehensive analysis," *Food Science and Nutrition*, vol. 9, no. 8, pp. 4364–4374, 2021.
- [17] W. A. Elkhateeb, G. M. Zaghlol, I. M. El-Garawani, E. F. Ahmed, M. E. Rateb, and A. E. Abdel Moneim, "Ganoderma applanatum secondary metabolites induced apoptosis through different pathways: in vivo and in vitro anticancer studies," *Biomedicine & Pharmacotherapy*, vol. 101, pp. 264–277, 2018.
- [18] Z. Liang, Z. Yuan, J. Guo et al., "Ganoderma lucidum polysaccharides prevent palmitic acid-evoked apoptosis and autophagy in intestinal porcine epithelial cell line via restoration of mitochondrial function and regulation of MAPK and AMPK/Akt/mTOR signaling pathway," *International Journal of Molecular Sciences*, vol. 20, no. 3, p. 478, 2019.
- [19] J. L. Lamaison, J. M. Polese, and C. Translations, *The Great Encyclopedia Of Mushrooms*, Koenemann, New York NY USA, 2005.
- [20] M. Rašková, L. Lacina, Z. Kejík et al., "The role of IL-6 in cancer cell invasiveness and metastasis—overview and therapeutic opportunities," *Cells*, vol. 11, no. 22, p. 3698, 2022.
- [21] A. Barbieri, V. Quagliariello, V. Del Vecchio et al., "Anti-cancer and anti-inflammatory properties of ganoderma lucidum extract effects on melanoma and triple-negative breast cancer treatment," *Nutrients*, vol. 9, no. 3, p. 210, 2017.
- [22] Q. X. Gan, J. Wang, J. Hu et al., "Modulation of apoptosis by plant polysaccharides for exerting anti-cancer effects: a review," *Frontiers in Pharmacology*, vol. 11, no. 5, p. 792, 2020.
- [23] M. Brentnall, L. Rodriguez-Menocal, R. L. De Guevara, E. Cepero, and L. H. Boise, "Caspase-9, caspase-3 and caspase-7 have distinct roles during intrinsic apoptosis," *BMC Cell Biology*, vol. 14, no. 1, p. 32, 2013.
- [24] T. Monkkinen and J. Debnath, "Inflammatory signaling cascades and autophagy in cancer," *Autophagy*, vol. 14, no. 2, pp. 190–198, 2018.
- [25] D. J. Han, J. B. Kim, S. Y. Park, M. G. Yang, and H. Kim, "Growth inhibition of hepatocellular carcinoma Huh7 cells by *Lactobacillus casei* extract," *Yonsei Medical Journal*, vol. 54, no. 5, pp. 1186–1193, 2013.
- [26] R. S. Y. Wong, "Apoptosis in cancer: from pathogenesis to treatment," *Journal of Experimental & Clinical Cancer Research*, vol. 30, no. 1, pp. 87–14, 2011.
- [27] B. B. Basnet, L. Liu, L. Bao, and H. Liu, "Current and future perspective on antimicrobial and anti-parasitic activities of *Ganoderma* sp.: an update," *Mycology*, vol. 8, no. 2, pp. 111–124, 2017.
- [28] S. E. Mansy, "Ganoderma: the mushroom of immortality," *Microbial Biosystems*, vol. 4, no. 1, pp. 45–57, 2019.
- [29] M. F. Ahmad, "Ganoderma lucidum: a rational pharmacological approach to surmount cancer," *Journal of Ethnopharmacology*, vol. 260, no. 5, Article ID 113047, 2020.
- [30] D. Cör, Ž. Knez, and M. K. Hrnčič, "Antitumour, antimicrobial, antioxidant and antiacetylcholinesterase effect of

- Ganoderma Lucidum terpenoids and polysaccharides: a review," *Molecules*, vol. 23, no. 3, pp. 1–21, 2018.
- [31] M. Wang and F. Yu, "Research progress on the anticancer activities and mechanisms of polysaccharides from ganoderma," *Frontiers in Pharmacology*, vol. 13, no. 7, pp. 891171–891216, 2022.
- [32] Y. Yu, L. Qian, N. Du, Y. Liu, X. Zhao, and X. Zhang, "Ganoderma lucidum polysaccharide enhances radiosensitivity of hepatocellular carcinoma cell line HepG2 through Akt signaling pathway," *Experimental and Therapeutic Medicine*, vol. 14, no. 6, pp. 5903–5907, 2017.
- [33] X. Hanyu, L. Lanyue, D. Miao, F. Wentao, C. Cangran, and S. Hui, "Effect of Ganoderma applanatum polysaccharides on MAPK/ERK pathway affecting autophagy in breast cancer MCF-7 cells," *International Journal of Biological Macromolecules*, vol. 146, pp. 353–362, 2020.
- [34] S. Hafeez, M. Urooj, S. Saleem et al., "BAD, a proapoptotic protein, escapes ERK/RSK phosphorylation in deguelin and siRNA-treated hela cells," *PLoS One*, vol. 11, no. 1, Article ID 145780, 2016.
- [35] S. Khazaei, N. M. Esa, V. Ramachandran et al., "In vitro antiproliferative and apoptosis inducing effect of Allium atroviolaceum bulb extract on breast, cervical, and liver cancer cells," *Frontiers in Pharmacology*, vol. 8, no. 1, p. 5, 2017.
- [36] A. Showalter, A. Limaye, J. L. Oyer et al., "Cytokines in immunogenic cell death: applications for cancer immunotherapy," *Cytokine*, vol. 97, no. 3, pp. 123–132, 2017.
- [37] H. Zhao, L. Wu, G. Yan et al., "Inflammation and tumor progression: signaling pathways and targeted intervention," *Signal Transduction and Targeted Therapy*, vol. 6, no. 1, p. 263, 2021.
- [38] A. M. K. Law, F. Valdes-mora, and D. Gallego-ortega, "Myeloid-derived suppressor cells as a therapeutic target for cancer," *Cells*, vol. 9, no. 3, p. 561, 2020.
- [39] B. J. Plotkin, I. M. Sigar, J. A. Swartzendruber, A. Kaminski, and J. Davis, "Differential expression of cytokines and receptor expression during anoxic growth," *BMC Research Notes*, vol. 11, no. 1, pp. 406–409, 2018.
- [40] N. Afroze, S. Pramodh, J. Shafarin et al., "Fisetin deters cell proliferation, induces apoptosis, alleviates oxidative stress and inflammation in human cancer cells, HeLa," *International Journal of Molecular Sciences*, vol. 23, no. 3, p. 1707, 2022.
- [41] M. Lambelet, L. F. Terra, M. Fukaya et al., "Dysfunctional autophagy following exposure to pro-inflammatory cytokines contributes to pancreatic β -cell apoptosis," *Cell Death & Disease*, vol. 9, no. 2, p. 96, 2018.
- [42] M. Redza-Dutordoir and D. A. Averill-Bates, "Activation of apoptosis signalling pathways by reactive oxygen species," *Biochimica et Biophysica Acta (BBA)- Molecular Cell Research*, vol. 1863, no. 12, pp. 2977–2992, 2016.
- [43] P. Li, L. Zhou, T. Zhao et al., "Caspase-9: structure, mechanisms and clinical application," *Oncotarget*, vol. 8, no. 14, pp. 23996–24008, 2017.
- [44] E. Dirican, H. Özcan, S. Karabulut Uzunçakmak, and U. Takım, "Evaluation expression of the caspase-3 and caspase-9 apoptotic genes in schizophrenia patients," *Clinical Psychopharmacology and Neuroscience*, vol. 21, no. 1, pp. 171–178, 2023.
- [45] Y. E. Hadisaputri, R. Andika, I. Sopyan et al., "Caspase cascade activation during apoptotic cell death of human lung carcinoma cells A549 induced by marine sponge *Callyspongia aerizusa*," *Drug Design, Development and Therapy*, vol. 15, pp. 1357–1368, 2021.
- [46] A. T. Kiddane, M. J. Kang, T. C. Ho et al., "Anticancer and apoptotic activity in cervical adenocarcinoma HeLa using crude extract of ganoderma applanatum," *Current Issues in Molecular Biology*, vol. 44, no. 3, pp. 1012–1026, 2022.
- [47] F. L. Hakkim, M. Al-Buloshi, and J. Achankunju, "Chemical composition and anti-proliferative effect of Oman's Ganoderma applanatum on breast cancer and cervical cancer cells," *Journal of Taibah University Medical Sciences*, vol. 11, no. 2, pp. 145–151, 2016.